Analysis of the Mechanical Characteristicsof Torsion Spring for Overrunning Clutch under Exponentially Distributed Loads and Continuous Boundary Constraints

Yuming Cao[1], Hongzhi Yan[1*], Bo Wen[1]
[1]State Key Laboratory of High Performance Complex Manufacturing, Central South University, Changsha, Hunan 410083, China
**Corresponding Author.*

Abstract

As a torsion element, the analysis of mechanical characteristics of torsion springs is critical to clutch design. This paper investigates the stress and deformation of torsion springs of spring-overrunning clutches by means of spatial curved beam theory, which fully takes account for the geometric nonlinearity and the initial curvature of the spring. The geometry of the spring before and after deformation is described by two Euler angles and three coordinate systems. Load and displacement constraints of torsion springs under real clutch operating conditions are analyzed and incorporated into the spring stress and deformation analysis. The numerical solution of this boundary value problem is carried out by the multiple shooting method and proved to be accurate by comparison. Moreover, this paper presents a method for calculating the torsional stiffness of springs, which can be applied to the analysis of torsional springs with irregular dimensions.

Keywords*: Spring overrunning clutch, Torsion spring, Spatial curved beam theory, Stress and deformation, Geometric nonlinearity, Torsional stiffness*

I. Introduction

The springoverrunning clutch is a mechanical device that can only transmit torque in one direction. It often used in aircraft, automobile, agricultural machinery, which is a key component of transmission system. Spring overrunning clutches have been widely used, but so far there has been little discussion about the stress and deformation of torsional springs in clutch engagement, and there are no accurate modeling and calculation methods available. In the open literature, only Lynwander, etc.(1) has calibrated the spring using the mechanical equations of an ordinary beam in the design of aviation spring overrunning clutch. In aviation, performance requirements for clutches are much higher, so there is a higher demand on clutch design, and it is necessary to further clarify the stress and deformation of springs under clutch operating conditions.

Figure 1 briefly illustrates the working principle of an overrunning clutch using a torsion spring. The spring expands radiallyto frictionally engage the input and output drum, transmitting torque from the inputto the output when the input member speed exceedsthe output member in a direction counter to the pitch of the spring coils. Otherwise, the coil spring contracts radially and disengages from the drum, allowing the output member to freely rotate. Figure 2 shows a cross-sectional view of the clutch. As a result of the interference fit, the teaser coils are always in contact with the cylindrical inner surface of the drum at both ends. As the clutch is not loaded, the rest of the coils havea uniform gap with the inner surface. When the input begins to transmit torque, the input drumgrips the teaser coilstwists and unwinds the entire coil spring, thereby causing the subsequent coil spring to unwind and expand outwardly against the cylindrical inner surfaces of the input and output clutch members.

Studies of the static properties of helical springs focus on natural frequencies and vibrations (Yildirim(2), Mottershead(3),XiongandTabarrok(4), Lee and Thompson(5)), stress-strain problems (Jiang and Henshell(6), Dammak(7), Taktak(8)), and are mainly conducted using finite element methods and transfer matrix methods.

However, the springs studied in these articles are only loaded with simple loads and simple boundary conditions. And little attention has been paid to the deformation of springs in the existing literature. Most of the literature considers springs with small deformations as the object of study, so the geometric nonlinearity exhibited by springs in large deformations is not fully considered.

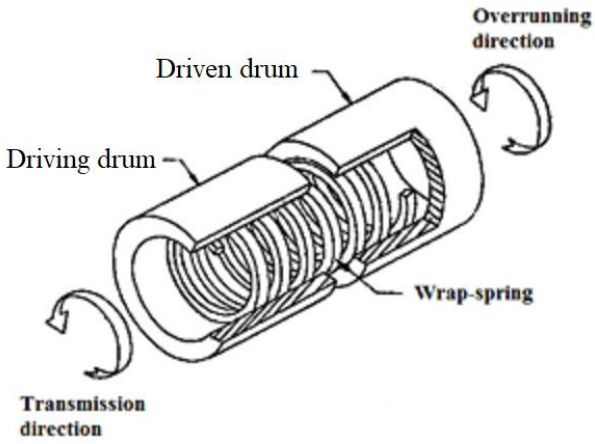

Fig. 1: Working principal diagram of spring overrunning clutch

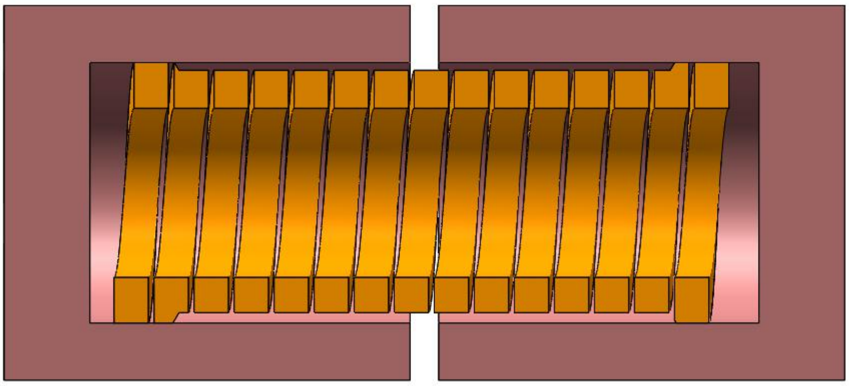

Fig.2: Cross-sectionalview of spring overrunning clutch

Since the springcoil has a much larger scalefor the length dimension than the other two dimensions, it is considered as aninitially curved and twisted beam. The displacement of an arbitrary cross section of a spatially curved beam in one direction is not only related by the strain in this direction, but also by the displacement of the rigid body in the other two directions and by the initial curvature. The spring is the torque transfer element of the overrunning clutch and is subjected to continuous and varying non-uniform loads distributed along the beam's length. During the operation of the expansion type spring clutch, the spring is continuously constrained by the drums in the cylinderdiameter direction. In analyzing the stress and deformation of springs, these complex loads and displacement constraints present challenges.

To derive the equations of motion of naturally curved and twisted beamconsidering geometric nonlinearities, it is common to use two or three successive Euler-like rotations to obtain the transformation matrix between the deformed and undeformed states(9-13).Houbolt and Brooks(14) derive the linear partial differential equation for the coupled bending and torsion of twisted nonuniform blades. Hodges and Dowell(15)develop a nonlinear theory to discuss the strain-displacement relations for long, slender beams. They derive the equations of motion for a rotating beam benefiting from Peter(16)'s contributions to transformation laws and strain-displacement relations.

ISSN: 0010-8189

However, coordinate transformations using three Euler angles result in asymmetric equations of motion, and the torsion-related angle does not represent the real twist angle even if only two Euler angles are used in the transformation. To solve this problem, Pai and Nayfeh(13) introduce the concept of virtual local rotationto derive fully nonlinear equations governing the motions along three perpendicular directions. Pai and Anderson(17) demonstrated the accuracy of the results of the spatial beam theory by experiments using flexible beams as objects.

Since the spring is continuously constrained by the drumin a certain direction, this is a complex super-stationary structural problem, and although the constraint is known, it cannot be solve00000d directly by Force Method due to the geometric nonlinearity of the spatial beam. This paper introducesthe nonlinear beam theory that fully accounts for initial curvatures and geometric nonlinearities to analyzes the stress and deformation of the helical spring in the clutch. The non-uniform load distribution caused by the drums on the helical spring during clutch engagement are also considered in this analysis.

II. Geometric modeling of spatial curved beam

The vector ***R***denotes the position of reference point on the neutral axis of an undeformed spatial curved beam. The *abc* coordinates represent a fixed global reference frame for indicating the position of each point in space. The *xyz*coordinatesis a local coordinate system describing the undeformed beam, whose *x*-axis is always tangent to the beam's neutral axis. The *ξηζ* coordinatesis a local coordinate system used to describe the deformed beam, with the*ξ*-axis representing the deformed neutral axis, and *η* and *ζ* axis representingthe deformed y-axis and z-axis, respectively.

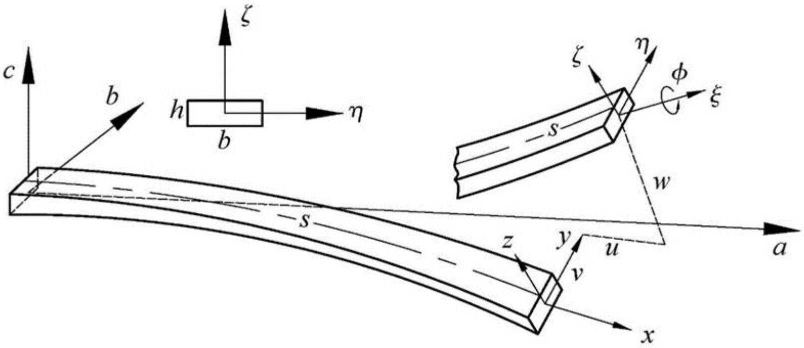

Fig. 3: Schematic diagram of deformation of a space beam with initial curvature

$$\boldsymbol{R} = A(s)\boldsymbol{i}_a + B(s)\boldsymbol{i}_b + C(s)\boldsymbol{i}_c \tag{1}$$

$\boldsymbol{i}_a$, $\boldsymbol{i}_b$, and $\boldsymbol{i}_c$ denote the unit vectors of the *abc* coordinate system. *s* denotes the undeformed arc length along the x-axis from the beam root to the observed reference point.

(1) The model of undeformed curve

$$\begin{Bmatrix} \boldsymbol{i}_x \\ \boldsymbol{i}_y \\ \boldsymbol{i}_z \end{Bmatrix} = [T^o] \begin{Bmatrix} \boldsymbol{i}_a \\ \boldsymbol{i}_b \\ \boldsymbol{i}_c \end{Bmatrix} \tag{2}$$

The *xyz*coordinate system consists of three-unit vectors, $\boldsymbol{i}_x$, $\boldsymbol{i}_y$, and $\boldsymbol{i}_z$.[T^o] is a transformation matrix that relates the coordinate system *abc* and *xyz*. Eq.can be obtained from the properties of the curve.

ISSN: 0010-8189

$$[T^o]' = \begin{bmatrix} A' & B' & C' \\ \cos\theta_{21} & \cos\theta_{22} & \cos\theta_{23} \\ T^o_{31} & T^o_{32} & T^o_{33} \end{bmatrix} \tag{3}$$

where $(\ )' = d(\ )/ds$; θ_{21}, θ_{22}, θ_{23} are the angles between the y-axis and a-axis, b-axis, and c-axis, respectively. According to the orthogonality of vectors $\boldsymbol{i}_z = \boldsymbol{i}_x \times \boldsymbol{i}_y$,

$$T^o_{31} = B'\cos\theta_{23} - C'\cos\theta_{22},\ T^o_{32} = C'\cos\theta_{21} - A'\cos\theta_{23},\ T^o_{33} = A'\cos\theta_{22} - B'\cos\theta_{21}$$

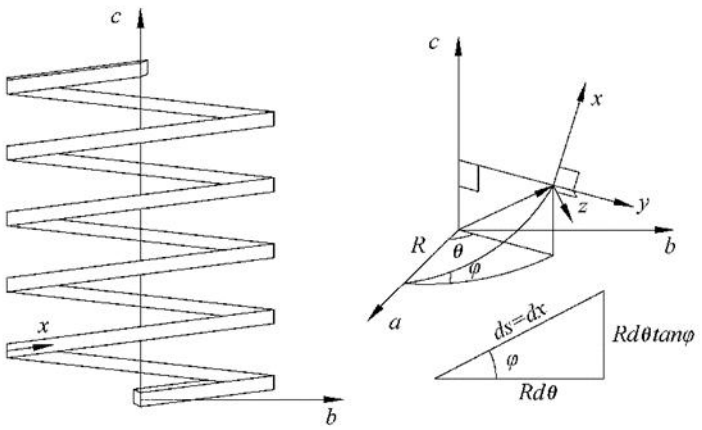

Fig. 4: The geometric relation between the coordinate systems abc and xyz

The parametric equation of helicalline is

$$\begin{cases} a = R\cos\theta \\ b = R\sin\theta \\ c = R\theta\tan\psi \end{cases} \tag{4}$$

The $[T^o]$ of helical line can be obtained from Eq. and

$$[T^o] = \begin{bmatrix} \cos\psi\sin\theta & \cos\psi\cos\theta & \sin\psi \\ \cos\theta & \sin\theta & 0 \\ \sin\psi\sin\theta & \sin\psi\cos\theta & -\cos\psi \end{bmatrix} \tag{5}$$

Using the Eq. and the orthonormality property

$$\frac{d}{ds}\begin{Bmatrix} \boldsymbol{i}_x \\ \boldsymbol{i}_y \\ \boldsymbol{i}_z \end{Bmatrix} = [k]\begin{Bmatrix} \boldsymbol{i}_x \\ \boldsymbol{i}_y \\ \boldsymbol{i}_z \end{Bmatrix} \tag{6}$$

where the initial curvature matrix [*k*] is given by

$$[k]=\begin{bmatrix} \boldsymbol{i}_x' \\ \boldsymbol{i}_y' \\ \boldsymbol{i}_z' \end{bmatrix}\begin{pmatrix} \boldsymbol{i}_x & \boldsymbol{i}_y & \boldsymbol{i}_z \end{pmatrix} = -\frac{d[T^o]}{ds}[T^o]^T \tag{7}$$

According to properties of orthogonal vector groups and the definition of torsion or curvature

$$k_1 \equiv \frac{d\boldsymbol{i}_y}{ds}\cdot \boldsymbol{i}_z = \sum_{i=1}^{3}\frac{dT^o_{2i}}{ds}T^o_{3i} \tag{8}$$

$$k_2 \equiv \frac{d\boldsymbol{i}_x}{ds}\cdot \boldsymbol{i}_z = -\sum_{i=1}^{3}\frac{dT^o_{1i}}{ds}T^o_{3i} \tag{9}$$

$$k_3 \equiv \frac{d\boldsymbol{i}_x}{ds}\cdot \boldsymbol{i}_y = \sum_{i=1}^{3}\frac{dT^o_{1i}}{ds}T^o_{2i} \tag{10}$$

where $k_1$is the initial torsion of curve, $k_2$and k_3 are the initial curvature of the curve in the xzplane and xyplane, respectively.

Then the initial torsion or curvature of helical linecan be obtained from eq and ~

$$k_1 = \frac{\cos\psi \sin\psi}{R},\ k_2 = \psi',\ k_3 = -\frac{\cos^2\psi}{R}$$

(2) The model of deformed curve

[*T*]is the coordinate transformation matrix from the *xyz* system to the *ξηζ* system.

$$\begin{bmatrix} \boldsymbol{i}_1 \\ \boldsymbol{i}_2 \\ \boldsymbol{i}_3 \end{bmatrix} = [T]\begin{bmatrix} \boldsymbol{i}_x \\ \boldsymbol{i}_y \\ \boldsymbol{i}_z \end{bmatrix} \tag{11}$$

The *ξηζ* coordinate system consists of three-unit vectors, $\boldsymbol{i}_1$, $\boldsymbol{i}_2$, and $\boldsymbol{i}_3$. [*T*] is a transformation matrix that relates the coordinate system *ξηζ* and *xyz*.

Two successive Euler angles *α* and *φ* are used to describe the rotation of the section from the undeformed position to the deformed position.The Euler angles *α* is generated by bending, and φ is related to the torsional deformation. Fig. 5 shows how the cross section is transformed from the xyz coordinate system to the ξηζ coordinate system by two rotations of the Euler angles.

Here, u,v, wrepresent the displacement of the reference point with respect to the x, y and z-axes, respectively Relate α to three displacements, which indicates the relationship between α and displacements.

ISSN: 0010-8189

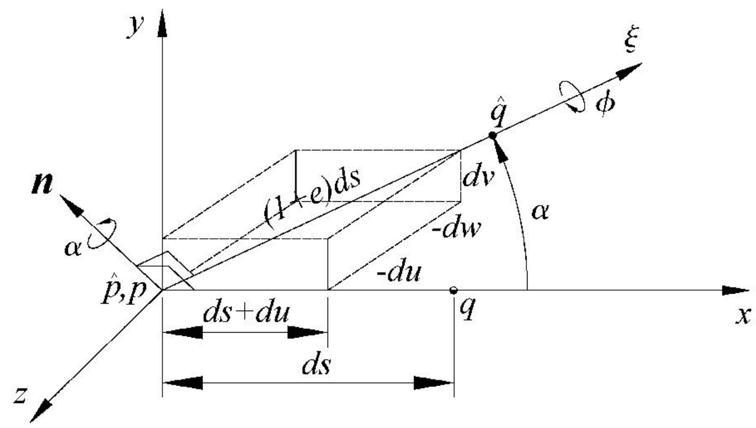

Fig. 5: Relationship between displacement of the neutral axis and the Euler angle

pq representsthe vector ofa section of undeformedbeam. At p, the displacement vector is$\boldsymbol{D}_1$, and at q, itis $\boldsymbol{D}_2$

$$\boldsymbol{D}_1 = u\boldsymbol{i}_x + v\boldsymbol{i}_y + w\boldsymbol{i}_z \tag{12}$$

$$\begin{aligned}\boldsymbol{D}_2 &= \boldsymbol{D}_1 + \frac{\delta \boldsymbol{D}_1}{\delta s} ds \\ &= \boldsymbol{D}_1 + [(u' - vk_3 + wk_2)\boldsymbol{i}_x + (v + uk_3 - wk_1)\boldsymbol{i}_y + (w - uk_2 + vk_1)\boldsymbol{i}_z]ds\end{aligned} \tag{13}$$

$\hat{p}$, $\hat{q}$ are the deformed reference point of p, q Hence, the vector of $\boldsymbol{pq}$ is deformed into $\hat{\boldsymbol{p}}\hat{\boldsymbol{q}}$

$$\begin{aligned}\hat{\boldsymbol{p}}\hat{\boldsymbol{q}} &= ds\boldsymbol{i}_x + \boldsymbol{D}_2 - \boldsymbol{D}_1 \\ &= [(1 + u' - vk_3 + wk_2)\boldsymbol{i}_x + (v + uk_3 - wk_1)\boldsymbol{i}_y + (w - uk_2 + vk_1)\boldsymbol{i}_z]ds\end{aligned} \tag{14}$$

Therefore

$$\boldsymbol{i}_1 = \frac{\hat{\boldsymbol{p}}\hat{\boldsymbol{q}}}{(1+e)ds} = T_{11}\boldsymbol{i}_x + T_{12}\boldsymbol{i}_y + T_{13}\boldsymbol{i}_z \tag{15}$$

$$T_{11} = \frac{1 + u' - vk_3 + wk_2}{1+e} \tag{16}$$

$$T_{12} = \frac{v' + uk_3 - wk_1}{1+e} \tag{17}$$

$$T_{13} = \frac{w' - uk_2 + vk_1}{1+e} \tag{18}$$

ISSN: 0010-8189

$$
\begin{aligned}
e &= \frac{\overline{\hat{p}\hat{q}} - ds}{ds} \\
&= \sqrt{(1+u' - vk_3 + wk_2)^2 + (v' + uk_3 - wk_1)^2 + (w' - uk_2 + vk_1)^2} - 1
\end{aligned} \tag{19}
$$

where e is the axial strain along the neutral axis ($\hat{\boldsymbol{p}}\hat{\boldsymbol{q}}$).

According to the relationship of the vector rotate, the elements of matrix $[T]$, T_{2i}, T_{3i}, can be represented in term of T_{11}, T_{12}, T_{13},ϕ.

$$T_{21} = -\cos\phi T_{12} - \sin\phi T_{13} \tag{20}$$

$$T_{22} = \cos\phi \left(T_{11} + \frac{T_{13}^2}{1+T_{11}} \right) - \sin\phi \frac{T_{12}T_{13}}{1+T_{11}} \tag{21}$$

$$T_{23} = \sin\phi \left(T_{11} + \frac{T_{12}^2}{1+T_{11}} \right) - \cos\phi \frac{T_{12}T_{13}}{1+T_{11}} \tag{22}$$

$$T_{31} = \sin\phi T_{12} - \cos\phi T_{13} \tag{23}$$

$$T_{32} = -\sin\phi \left(T_{11} + \frac{T_{13}^2}{1+T_{11}} \right) - \cos\phi \frac{T_{12}T_{13}}{1+T_{11}} \tag{24}$$

$$T_{33} = \cos\phi \left(T_{11} + \frac{T_{12}^2}{1+T_{11}} \right) + \sin\phi \frac{T_{12}T_{13}}{1+T_{11}} \tag{25}$$

Differentiating eq with respect to s and using Eq. yield

$$\frac{\partial}{\partial s} \begin{Bmatrix} \boldsymbol{i}_1 \\ \boldsymbol{i}_2 \\ \boldsymbol{i}_3 \end{Bmatrix} = [K] \begin{Bmatrix} \boldsymbol{i}_1 \\ \boldsymbol{i}_2 \\ \boldsymbol{i}_3 \end{Bmatrix} \tag{26}$$

$$
\begin{aligned}
[K] &\equiv \begin{bmatrix} \boldsymbol{i}_1' \cdot \boldsymbol{i}_1 & \boldsymbol{i}_1' \cdot \boldsymbol{i}_2 & \boldsymbol{i}_1' \cdot \boldsymbol{i}_3 \\ \boldsymbol{i}_2' \cdot \boldsymbol{i}_1 & \boldsymbol{i}_2' \cdot \boldsymbol{i}_2 & \boldsymbol{i}_2' \cdot \boldsymbol{i}_3 \\ \boldsymbol{i}_3' \cdot \boldsymbol{i}_1 & \boldsymbol{i}_3' \cdot \boldsymbol{i}_2 & \boldsymbol{i}_3' \cdot \boldsymbol{i}_3 \end{bmatrix} = \begin{bmatrix} 0 & \rho_3 & \rho_2 \\ \rho_3 & 0 & \rho_1 \\ \rho_2 & \rho_1 & 0 \end{bmatrix} \\
&= [T]'[T]^T + [T][k][T]^T
\end{aligned} \tag{27}
$$

where ρ_1 is the torsion of deformed curve, ρ_2 and ρ_3 are the curvature of deformed curve in the $\xi\zeta$ plane and $\xi\eta$ plane, respectively.

it can obtain that

ISSN: 0010-8189

$$\rho_1 \equiv \boldsymbol{i}_2' \cdot \boldsymbol{i}_3 = \phi' + \frac{1}{(1+e)(1+T_{11})}\left[T_{13}(v' + k_3u - k_1w)' - T_{12}(w' - k_2u + k_1v)'\right] + T_{11}k_1 + T_{12}k_2 + T_{13}k_3 \tag{28}$$

$$\rho_2 \equiv -\boldsymbol{i}_1' \cdot \boldsymbol{i}_3 = \frac{-1}{(1+e)}\left[T_{31}(u' - k_3v + k_2w)' + T_{32}(v' + k_3u - k_1w)' + T_{33}(w' - k_2u + k_1v)'\right] + T_{21}k_1 + T_{22}k_2 + T_{23}k_3 \tag{29}$$

$$\rho_3 \equiv \boldsymbol{i}_1' \cdot \boldsymbol{i}_2 = \frac{1}{(1+e)}\left[T_{21}(u' - k_3v + k_2w)' + T_{22}(v' + k_3u - k_1w)' + T_{23}(w' - k_2u + k_1v)'\right] + T_{31}k_1 + T_{32}k_2 + T_{33}k_3 \tag{30}$$

Eq.~ describe the geometry of deformed beam by torsion and curvature.

(3) Variations of strain and curvatures

$\delta\theta_1$, $\delta\theta_2$, $\delta\theta_3$are virtual rotation angles with respect to the axes ξ, η, ζ, respectively. Variations of unit vectors $\boldsymbol{i}_k$ result from virtual rotations of the observed cross-section.

$$\begin{Bmatrix} \delta\boldsymbol{i}_1 \\ \delta\boldsymbol{i}_2 \\ \delta\boldsymbol{i}_3 \end{Bmatrix} = \begin{bmatrix} 0 & \delta\theta_3 & -\delta\theta_2 \\ -\delta\theta_3 & 0 & \delta\theta_1 \\ \delta\theta_2 & -\delta\theta_1 & 0 \end{bmatrix} \begin{Bmatrix} \boldsymbol{i}_1 \\ \boldsymbol{i}_2 \\ \boldsymbol{i}_3 \end{Bmatrix} \tag{31}$$

The variation of curvature can be obtained by variational and integral calculations of curvatures

$$\begin{Bmatrix} \delta\rho_1 \\ \delta\rho_2 \\ \delta\rho_3 \end{Bmatrix} = \begin{Bmatrix} (\delta\theta_1)' \\ (\delta\theta_2)' \\ (\delta\theta_3)' \end{Bmatrix} - [K]\begin{Bmatrix} \delta\theta_1 \\ \delta\theta_2 \\ \delta\theta_3 \end{Bmatrix} \tag{32}$$

III. Nonlinear equation of motion

The extended Hamilton principle, as well as the local engineering stresses and strains, and the new interpretation and manipulation of orthogonal virtual rotations, are used to obtain six fully nonlinear equations of motion(13).The governing partial differential equations can be derived to be

$$\begin{Bmatrix} F_1' \\ F_2' \\ F_3' \end{Bmatrix} - [K]\begin{Bmatrix} F_1 \\ F_2 \\ F_3 \end{Bmatrix} + [T]\begin{Bmatrix} q_1 \\ q_2 \\ q_3 \end{Bmatrix} = \begin{Bmatrix} 0 \\ 0 \\ 0 \end{Bmatrix} \tag{33}$$

$$\begin{Bmatrix} M_1' \\ M_2' \\ M_3' \end{Bmatrix} - [K]\begin{Bmatrix} M_1 \\ M_2 \\ M_3 \end{Bmatrix} + (1+e)\begin{Bmatrix} 0 \\ -F_3 \\ F_2 \end{Bmatrix} = -\begin{Bmatrix} q_4 \\ 0 \\ 0 \end{Bmatrix} \tag{34}$$

$$F_2 = -\frac{1}{1+e}(M_3' + M_2\rho_1 - M_1\rho_2) \tag{35}$$

$$F_3 = \frac{1}{1+e}(M_2' - M_3\rho_1 + M_1\rho_3) \tag{36}$$

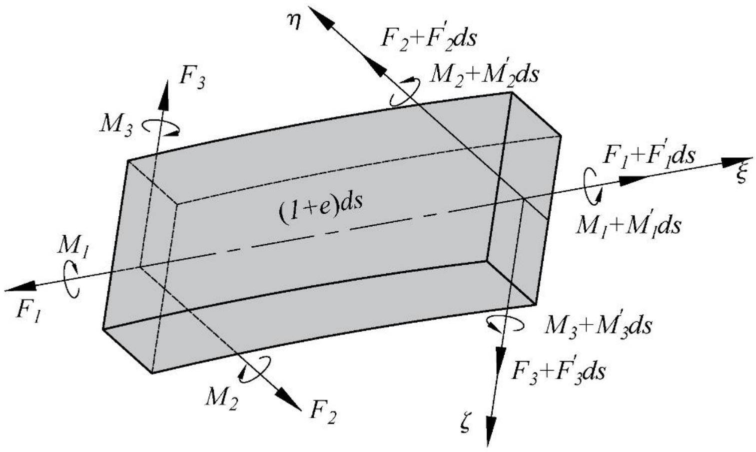

Fig.6: Differential beam element subjected to stress resultants and moments

Fig.6 illustratesa differential beam element subjected to stress resultants and moments.F_i; are the stress resultants, and M_i, are the stress moments. F_2 and $F_3$are transverse shear resultants, which can be represented in terms of stress moments and their derivatives by using Eq. q_1, q_2 and q_3 are distributed external forces acting along axes x, y and z, respectively, and q_4, q_5 and q_6 are distributed external moments acting along axes *ξ, η,* and *ζ*, respectively.

$$F_1 = \int_A \sigma_{11}\,dydz \tag{37}$$

$$M_1 = \int_A \left(y\sigma_{13} - z\sigma_{12}\right) dydz \tag{38}$$

$$M_2 = \int_A z\sigma_{11}\,dydz \tag{39}$$

$$M_3 = \int_A -y\sigma_{11}\,dydz \tag{40}$$

where A denotes the cross-section area, σ_{ij} are Jaumann stress.

$$\begin{Bmatrix} \sigma_{11} \\ \sigma_{12} \\ \sigma_{13} \end{Bmatrix} = \begin{bmatrix} E & & \\ & G & \\ & & G \end{bmatrix} \begin{Bmatrix} \varepsilon_{11} \\ \varepsilon_{12} \\ \varepsilon_{13} \end{Bmatrix} \tag{41}$$

where ε_{ij} are Jaumann strains, E is Young's modulus, G is shear modulus and $\sigma_{22}=\sigma_{33}=\sigma_{23}=0$ is assumed. The strain-displacement relations are

$$\varepsilon_{11} = e + z\bar{\rho}_2 - y\bar{\rho}_3 \tag{42}$$

$$\varepsilon_{12} = -z\bar{\rho}_1 \tag{43}$$

$$\varepsilon_{13} = y\bar{\rho}_1 \tag{44}$$

where $\bar{\rho}_i = \rho_i - k_i$

Substituting Equations~ into Eq., it can be obtained that

$$\begin{Bmatrix} F_1 \\ M_1 \\ M_2 \\ M_3 \end{Bmatrix} = \begin{bmatrix} EA & & & \\ & GI_p & & \\ & & EI_2 & \\ & & & EI_3 \end{bmatrix} \begin{Bmatrix} e \\ \bar{\rho}_1 \\ \bar{\rho}_2 \\ \bar{\rho}_3 \end{Bmatrix} \tag{45}$$

where $I_2 = \frac{1}{12}hb^3$, $I_3 = \frac{1}{12}bh^3$, $I_p = I_2 + I_3$ .b represents the dimension of the cross-section (yz-plane)in the z-axis direction, and h is the dimension in the y-axis direction.

IV. Load and boundary condition analysis

(1) Analysis of loads

Take any element of the spring coil for force analysis as shown in Fig.7. The spring element is subjected to pressure and friction from the drum. The center Angle of the element spring is $d\varphi$, df and dN are respectively the friction and pressure from the drum to the element of spring. P is the equivalent concentrated force produced by moment of couple T on the element. dP and dT present the increments of the force and moment, respectively.

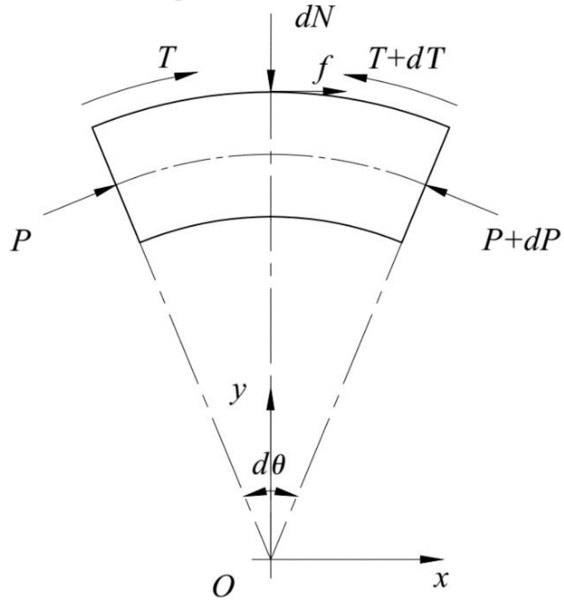

Fig. 7: Force diagram of spring element

ISSN: 0010-8189

According to the moment and force balance of element, the following two equations (2.5, 2.6) are established.

$$dN = P\sin\frac{d\theta}{2} + (P + dP)\sin\frac{d\theta}{2} \tag{46}$$

$$T + Rdf = T + dT \tag{47}$$

Since the center angle of the element is very small, it can be taken $\sin d\theta \approx d\theta$ and $dP\sin\frac{d\theta}{2} \approx 0$. From the definition of moment and friction force, equations (2.7) and (2.8) can be obtained, respectively.

$$P = \frac{T}{R} \tag{48}$$

$$df = udN \tag{49}$$

Through the equation (2.5) and (2.7), equation (2.9) can be obtained.

$$dN = \frac{T}{R}d\theta \tag{50}$$

Combined the equation (2.6), (2.8) and (2.9), the differential equation (2.10) can be gotten. There is an initial energizing moment due to the interference fit of energizing coils, that is, $T=T_0$ when $\theta = 0$ .By integrating the differential equation (2.10),the equation (2.11) can be obtained.

$$\int_0^{\theta} \mu d\varphi = \int_{T_0}^{T} \frac{dT}{T} \tag{51}$$

$$T = T_0 e^{\mu\theta} \tag{52}$$

The equation , which shows the relationship between the torque transmitted by clutch and the pole Angle of the spring in contact with the inner surface, shows that the torque increases exponentially with the polar Angle. μ represents the coefficient of friction between the outer surface of the spring and the inner surface of the drum.

It can be derived from equations and that applied pressure and friction are both exponentially distributed loads, and their load concentration functions are as shown in equations and .

$$q_N = \frac{dN}{ds} = \frac{T_0 e^{\mu\theta}}{R^2} \tag{53}$$

$$q_f = \frac{df}{ds} = \frac{\mu T_0 e^{\mu\theta}}{R^2} \tag{54}$$

ds is arc length of element, $ds = Rd\varphi$.

ISSN: 0010-8189

Thus, combining the spring geometry gives

$$q_1 = \frac{\mu T_0 e^{\mu\theta}}{R^2}\cos\psi, q_2 = \frac{T_0 e^{\mu\theta}}{R^2}, q_3 = \frac{\mu T_0 e^{\mu\theta}}{R^2}\sin\psi$$

(2) Analysis of boundary conditions

Since the spring is a symmetric structure about the middle section (y-z plane), it is possible to calculate it considering only one half of the structure to reduce the calculation volume. The arc length of the half of spring coil is set to L, let the middle section s = L, the free end s = 0.

Based on structural symmetry and its own characteristics, two ends have the following boundary conditions:

$$\begin{aligned} &\text{at s=0: } F_1 = F_3 = M_1 = M_2 = M_3 = v = 0 \\ &\text{at s=L: } T_{11} = 1, T_{12} = T_{13} = \phi = u = w = 0, v = \Delta D \end{aligned} \tag{55}$$

In addition, the boundary conditions of spring coils are $v(s) = \Delta D (0 < s < L)$.

V. Numerical solution and discussion

Expanding the equation yields

$$F_1' = \rho_3 F_2 - \rho_2 F_3 - T_{11} q_1 - T_{12} q_2 - T_{13} q_3 \tag{56}$$

$$F_2' = \rho_1 F_3 - \rho_3 F_1 - T_{21} q_1 - T_{22} q_2 - T_{23} q_3 \tag{57}$$

$$F_3' = \rho_2 F_1 - \rho_1 F_2 - T_{31} q_1 - T_{32} q_2 - T_{33} q_3 \tag{58}$$

$$M_1' = \rho_3 M_2 - \rho_2 M_3 - q_4 \tag{59}$$

$$M_2' = \rho_1 M_3 - \rho_2 M_1 + (1+e) F_3 - q_5 \tag{60}$$

$$M_3' = \rho_2 M_1 - \rho_1 M_2 - (1+e) F_2 - q_6 \tag{61}$$

It follows by the Eq. that

$$T_{11}' = \rho_3 T_{21} - \rho_2 T_{31} + T_{12} k_3 - T_{13} k_2 \tag{62}$$

$$T_{12}' = \rho_3 T_{22} - \rho_2 T_{32} + T_{13} k_1 - T_{11} k_3 \tag{63}$$

$$T_{13}' = \rho_3 T_{23} - \rho_2 T_{33} + T_{11} k_2 - T_{12} k_1 \tag{64}$$

Substituting Eq. into Eq. yields

$$\phi' = \rho_1 - T_{11}k_1 - T_{12}k_2 - T_{13}k_3 - \frac{T_{13}}{1+T_{11}}(\rho_3 T_{22} - \rho_2 T_{32} + T_{13}k_1 - T_{11}k_3) + \frac{T_{12}}{1+T_{11}}(\rho_3 T_{23} - \rho_2 T_{33} + T_{11}k_2 - T_{12}k_1) \tag{65}$$

It can obtained from Eq.~ that

$$u' = -1 + vk_3 - wk_2 + (1+e)T_{11} \tag{66}$$

$$v' = wk_1 - uk_3 + (1+e)T_{12} \tag{67}$$

$$w' = uk_2 - vk_1 + (1+e)T_{13} \tag{68}$$

F_1, F_2, F_3, M_1, M_2, M_3, T_{11}, T_{12}, T_{13}, ϕ, u,v, $w$are used as 13 independent variables, and the 13 first-order ordinary differential equations ~are solved numerically using the multiple shooting method.

Table 1: Physical Properties of Torsion Springs Used in Clutch

Parameter(unit)	Value
E (GPa)	2.11e2
ν	0.32
b (mm)	10
h (mm)	8
ΔD (mm)	0.1
R (mm)	23
N	17.5
ψ *(degree)*	5
μ	0.1

ν *is the Poisson's ratio. N* means half number of coils of the spring, so the maximum value of θ(Polar Angle) in equation is $2N\pi$.

The following results are calculated from a load loading with a torque of 1200 N·m (i.e.T_0 = 0.02N·m). Fig.8(a) to(f) show the distribution of the stress resultants and moments of the spring on the length scale (0 to L), where the horizontal coordinates are represented by the polar angle ($\theta = s/R$) .Fig.11 shows the displacements in the x-axial and z-axial directions, i.e., u and w, generated on each element, respectively.

ISSN: 0010-8189

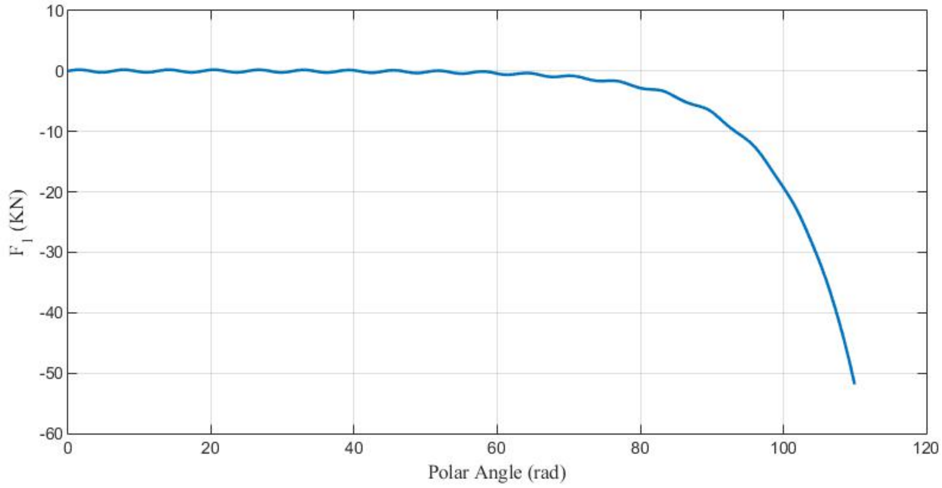

(a) F_1

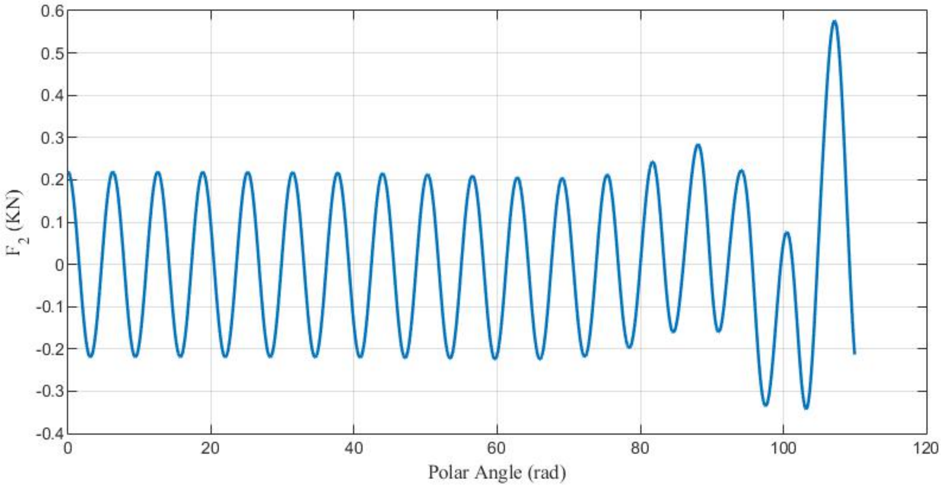

(b) F_2

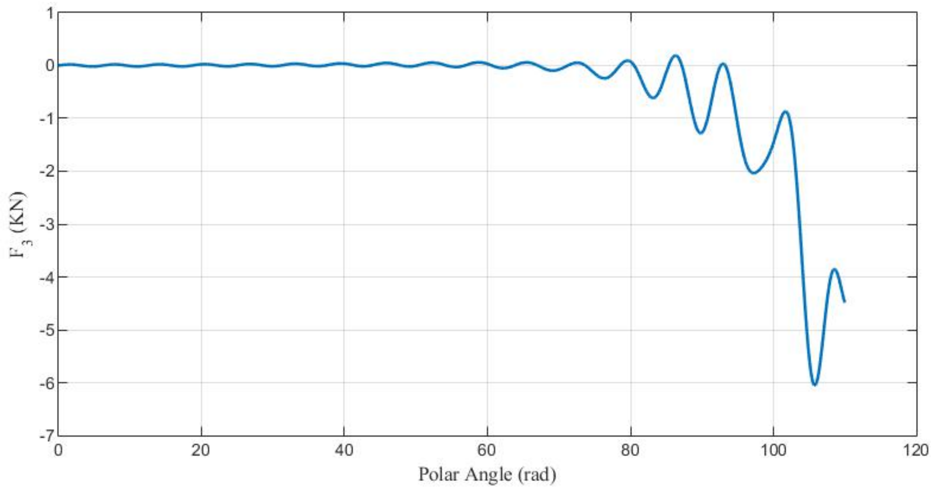

ISSN: 0010-8189

(c) F_3

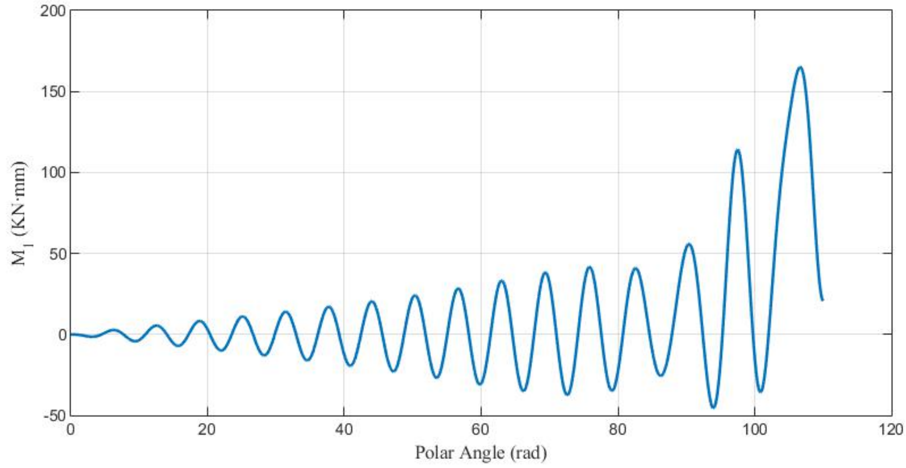
200
150
100
50
0
-50
0
20
40
60
80
100
120
M_1 (KN·mm)
Polar Angle (rad)

(d) M_1

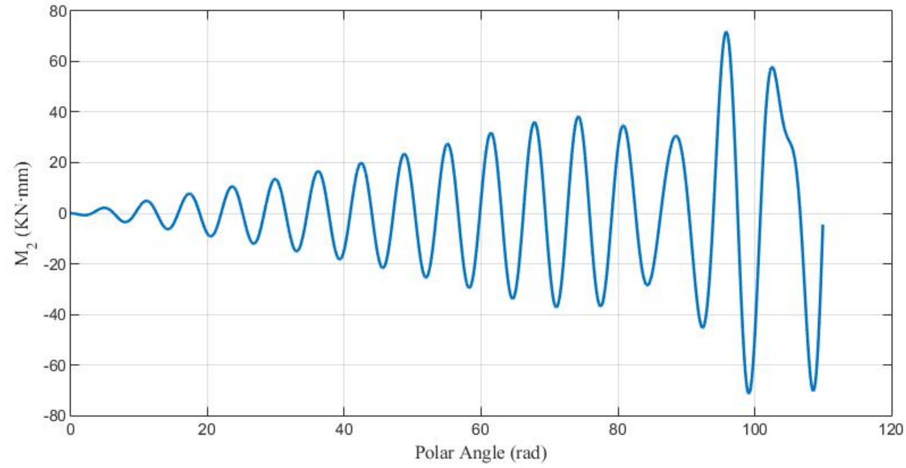
80
60
40
20
0
-20
-40
-60
-80
0
20
40
60
80
100
120
M_2 (KN·mm)
Polar Angle (rad)

(e) M_2

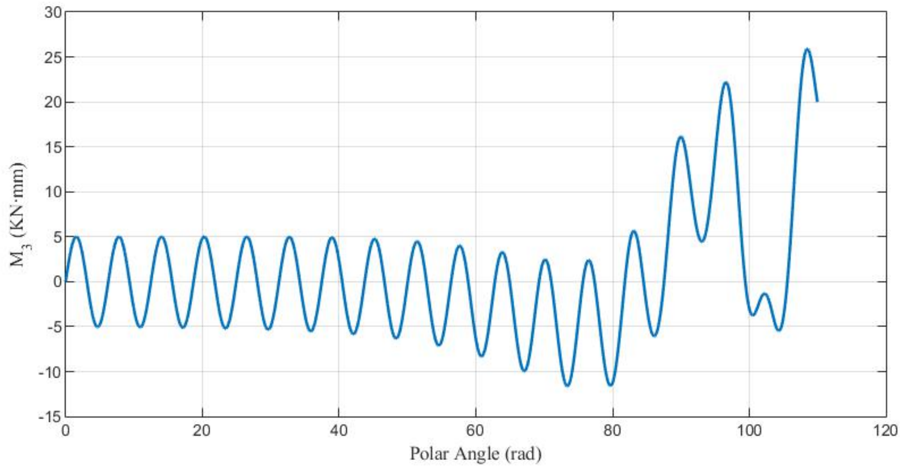

(f) M_3

Fig. 8: Distribution of stressresultants and moments in each direction

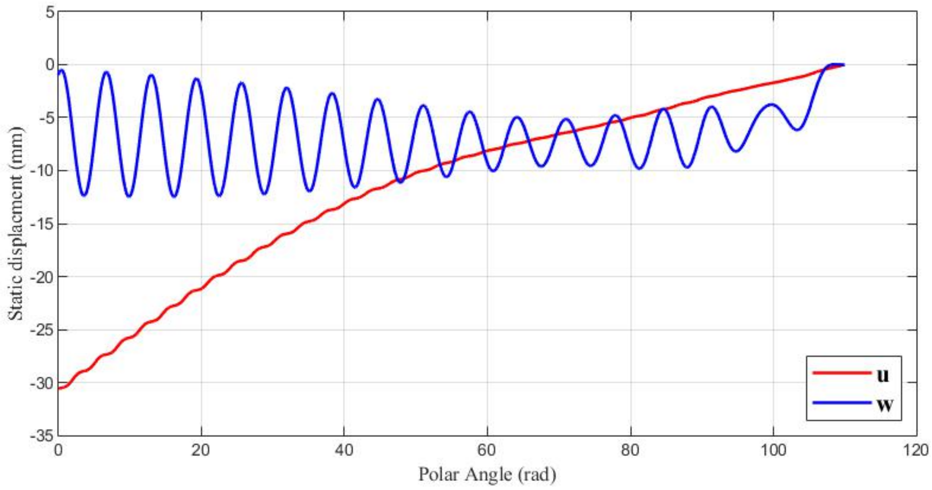

Fig.9: The static displacement of each element

F_2 and F_3 increase in an exponential manner with the pole angle. Where F_1 has the largest value, exceeding 51 KN in the middle section. Although there is a constant displacement boundary constraint in the y-direction, the F_2 and M_3 in the direction associated with it still vary to varying degrees. Stress resultants and moments and curvature increments have the highest values near the middle section of the spring, so the deformation is the greatest there. In the x and z directions, there are no significant differences in the displacements produced by the elements at different positions of the spring.

The torsion process of the overrunning clutch was simulated using ABAQUS finite element software, and the values of F_1 at each section were extracted from the results and compared with the numerical solution. From the comparison, the difference between the numerical solution and the results of the finite element software is very small as seen in Fig.10, which can prove the accuracy of the method.

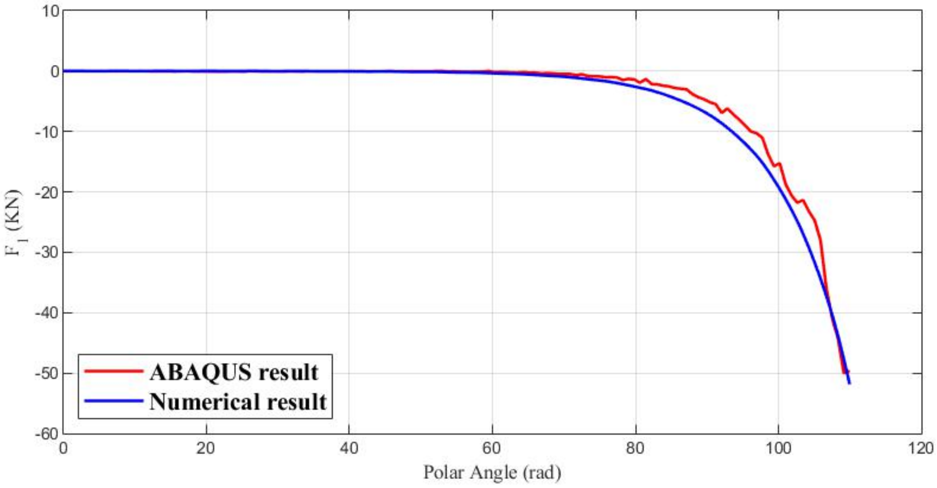

Fig.10: Comparison of numerical results with ABAQUS results

The calculated deformation of each section of the spring coil is used to calculate the torsional deformation of the entire spring using geometric relationships, which further allows the torsional stiffness of the spring to be found.

VI. Calculation of spring torsional stiffness

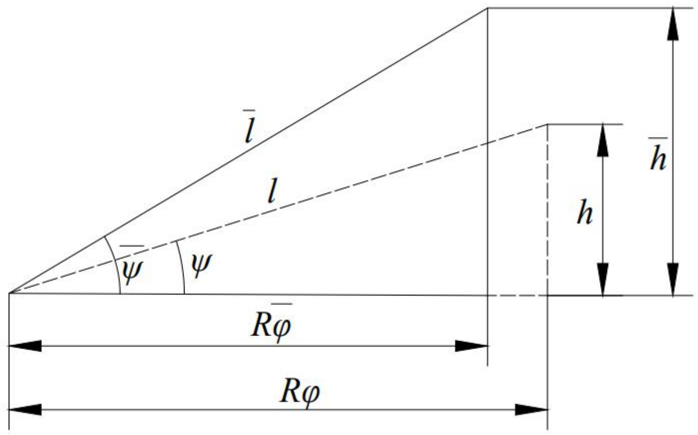

Fig.11: Comparison of numerical results with ABAQUS results

$$\Delta h = \Delta u \sin\psi - \Delta w \cos\psi \tag{69}$$

Δu and $\Delta w$are the displacements of the spring wire in the x-axis and z-axis directions of the local coordinate system, respectively. Δh is the displacement of the spring coil in the direction of the c-axis of the global coordinate system (*abc*).The expression for the geometric relationship before and after the deformation of a section of spring coil is represented by equations ~.

$$\overline{h} = h + \Delta h \tag{70}$$

$$\overline{l} = l + e \tag{71}$$

$$\bar{R} = R + \Delta v \tag{72}$$

$$\bar{\psi} = arc\sin\left(\frac{\bar{h}}{\bar{l}}\right) \tag{73}$$

As shown in the Fig.12, l and $\bar{l}$ are the lengths of a section of spring coil before and after deformation respectively. ψ and $\bar{\psi}$ are the helix lift angles of a section of spring coil before and after deformation respectively. R and $\bar{R}$ are the cylindrical radius of a section of the spring before and after deformation respectively. Δv is the displacement of the spring coil in the direction of the y-axis of the local coordinate system. The geometric relationship described in Fig. 12 shows that the value of the change in polar angle produced before and after the deformation of a section of spring coil is

$$\Delta\varphi = \frac{\bar{l}\cos\bar{\psi}}{\bar{R}} - \frac{l\cos\psi}{R} \tag{74}$$

The torsion angle ϕ of the entire spring is therefore the sum of the changes in the polar angles $\Delta\varphi$ of the individual sections of the spring coil.

$$\phi = \sum_{m=1}^{Ne} \Delta\varphi_m \tag{75}$$

The torsional stiffness of a spring can be obtained from the definition by the following equation

$$k_t = \frac{\Delta T_e}{2\Delta\phi} \tag{76}$$

T_e=596$N \cdot m$ and 894$N \cdot m$ are input into the system of equations for solution, and the torsion angles φ are 1.9321 *rad* and 1.7719 *rad* respectively, so the torsional stiffness k_t can be calculated as 1.8605e3 N·m/rad according to the equation.

VII. Conclusion

It is necessary to determine the spring's static characteristics under realistic operating conditions in order to provide theoretical basis for clutch design. To estimate the stress and deformation of the spring under realistic operating conditions, the geometric nonlinearity of the spring is fully considered in this paper, and realistic load and displacement constraints are applied to the torsion spring in the clutch. The paper uses a two-node curved beam element to model the spring geometries accurately. Three coordinate systems are established to represent the geometry of the undeformed and deformed spring, and then uses variational methods to determine virtual displacement and deformation of the element. In the end, the problem is converted into 13 nonlinear ordinary differential equations by applying spatial curved beam theory. Multiple shooting method is used to solve this boundary value problem, and validity and accuracy of the results are proven. The paper addresses the problem that the deformation of springs subjected to complex loads cannot be calculated and proposes a torsional stiffness calculation for springs that can be applied to cylindrical springs of various parameters.

Acknowledgements

The authors gratefully acknowledge the support of the National Natural Science Foundation of China (NSFC) through Grants no. 51575533 and no.51805555, Key Project of Research and Development Plan of Hunan Province (2015JC3007).

References

[1] Lynwander P, Meyer AG, Chachakis S. Spring Overriding Aircraft Clutch. U. S. Army R & D Laboratory; 1973. Report No.: AD766309.

[2] Yildirim V. Axial Static Load Dependence Free Vibration Analysis of Helical Springs Based on the Theory of Spatially Curved Bars. Latin American Journal of Solids and Structures. 2016;13(15):2852-75.

[3] Mottershead JE. Finite elements for dynamical analysis of helical rods. International Journal of Mechanical Sciences. 1980;22(5):267-83.

[4] Xiong Y, Tabarrok B. A finite element model for the vibration of spatial rods under various applied loads. International Journal of Mechanical Sciences. 1992;34(1):41-51.

[5] Lee J, Thompson DJ. Dynamic Stiffness Formulation, Free Vibration and Wave Motion of Helical Springs. Journal of Sound and Vibration. 2001;239(2):297-320.

[6] Jiang WG, Henshall JL. A novel finite element model for helical springs. Finite Elements in Analysis and Design. 2000;35(4):363-77.

[7] Fakhreddine D, Mohamed T, Said A, Abderrazek D, Mohamed H. Finite element method for the stress analysis of isotropic cylindrical helical spring. European Journal of Mechanics - A/Solids. 2005;24(6):1068-78.

[8] Taktak M, Dammak F, Abid S, Haddar M. A finite element for dynamic analysis of a cylindrical isotropic helical spring. Journal of Mechanics of Materials and Structures. 2008;3(4):641-58.

[9] Bauchau OA, Hong CH. Large displacement analysis of naturally curved and twisted composite beams. AIAA Journal. 1987;25(11):1469-75.

[10] Rosen A, Rand O. A general model of the dynamics of moving and rotating rods. Computers & Structures. 1985;21(3):543-61.

[11] Alkire K. An Analysis of Rotor Blade Twist Variables Associated with Different Euler Sequences and Pretwist Treatments. NASA Ames Research Center Moffett Field; 1984. Contract No.: 19840018625.

[12] Pai PF, Nayfeh AH. Three-Dimensional Nonlinear Vibrations of Composite Beams - Ⅰ. Equations of Motion. Nonlinear Dynamics. 1990;1(6):477-502.

[13] Pai PF, Nayfeh AH. A fully nonlinear theory of curved and twisted composite rotor blades accounting for warpings and three-dimensional stress effects. International Journal of Solids & Structures. 1994;31(9):1309-40.

[14] Houbolt JC, Brooks GW. Differential equations of motion for combined flapwise bending, chordwise bending, and torsion of twisted nonuniform rotor blades. Langley Aeronautical Laboratory Langley Field, Va. ; 1957. Report No.: NACA-TN-3905 Contract No.: 19930092334.

[15] Hodges DH, Dowell EH. Nonlinear equations of motion for the elastic bending and torsion of twisted nonuniform rotor blades. NASA Technical Note (TN). 1974. Report No.: D-7818 Contract No.: 19750005242.

[16] Peters DA. The Effect of Principal Bending Curvature on the Lateral Buckling of Uniform Slender Beams. Journal of Applied Mechanics. 1977;44(2):311-6.

[17] Pai PF, Anderson TJ, Wheater EA. Large-deformation tests and total-Lagrangian finite-element analyses of flexible beams. International Journal of Solids and Structures. 2000;37(21):2951-80.